Appendix A

On The Rotation Axis of the Sun

In interpreting measurements of solar velocities, it is crucial to know the direction of the Sun's axis of rotation for each observation. The "known" axis of solar rotation that is used almost universally today was determined almost 150 years ago (Carrington, 1863) by observing the motions of sunspots recorded on photographic plates at a ground-based observatory[1]. Although Carrington did not offer an estimate of the uncertainty in his proposed standard, it seems unlikely that the error was less than about a tenth of a degree. Subsequent researchers have attempted to improve on the accuracy of this measurement, with varying results. This appendix presents a new measurement which may offer the most accurate determination yet, and compares the results with those obtained by other researchers in the last one hundred years. Finally, it is proposed that the set of more modern measurements be used to adopt a new standard for the Sun's axis of rotation.

[1]It is interesting to note that the observations required to make this calculation were available at least two hundred years earlier (see Eddy *et al.* (1976)

A.1 The Coordinate System: i and Ω

Consider the representation of the Sun in figure A.1[2]. The great circle ΥEN is the intersection of the plane of the ecliptic (the plane of the Earth's orbit) with the solar surface. The point C defines the center of the sphere, and CK is perpendicular to the ecliptic. The point Υ is defined such that a straight line drawn from C to Υ points in the direction of the vernal equinox; this is the reference direction from which celestial longitudes are measured. The line joining C and the Earth cuts the sphere at E, and the plane defined by CK and CT, perpendicular to CE, is defined as the plane of the disk. The heliocentric ecliptic longitude of the Earth is ΥE; the geocentric longitude of the Sun is denoted by $\eta = \Upsilon E + 180°$.

The Sun rotates around an axis CP, where P is the north pole of the Sun. The great circle perpendicular to this axis is the solar equator, of which the arc NJ is a section. The inclination of the solar equator to the ecliptic (the angle JNE in figure A.1) is denoted by i. The point N is the ascending node of the solar equator on the ecliptic plane, and its longitude ΥN is given the symbol Ω. The values of i and Ω completely determine the Sun's rotation axis. The standard values used by the astronomical community are those determined by Carrington (1863), namely

$$\begin{aligned} i_c &= 7.25°, \\ \Omega_c &= 73.67° + 0.013958°(t - 1850.0), \end{aligned} \tag{A.1}$$

where t is expressed in years. The value of Ω increases slowly due to precession.

The point E will be seen as the center of the disk; the latitude of this point must be known in order to correctly interpret the measured velocities. This latitude is denoted by B_0. For the spherical triangle defined by PEN,

[2] The notation and description in this section borrow heavily from Smart (1977). It is included here so that the reader need not make reference to that work.

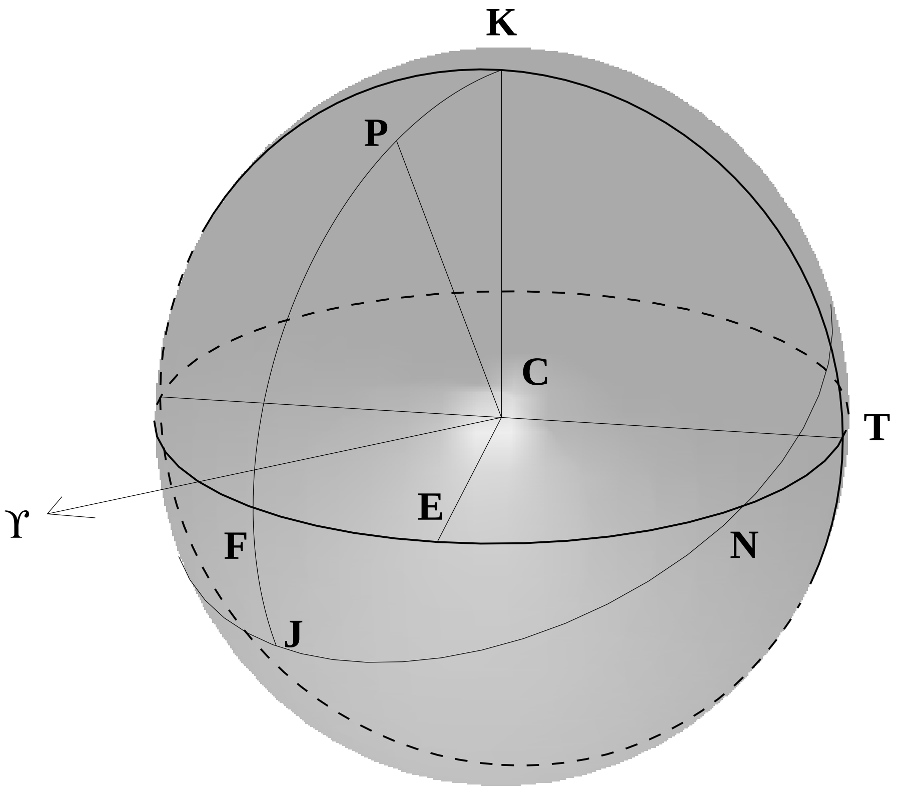

Figure A.1: The geometry of the coordinate system used in measuring solar positions. The line CP represents the rotation axis of the Sun; the axis CK is the pole of the ecliptic. The inclination (angle KCP) is exaggerated. Other symbols are explained in the text.

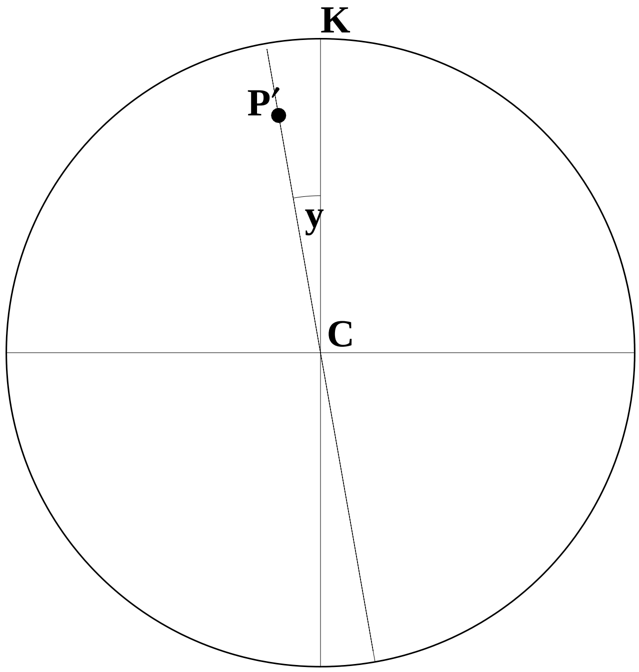

Figure A.2: The angle denoted by y is the *effective position angle* of the solar image taken by MDI. The point P' is the projection of the north pole of the Sun into the plane of the image.

$$
\begin{aligned}
PN &= 90°, \\
PE &= 90° - B_0, \\
EN &= \Omega - \eta - 180°, \\
\angle PNE &= 90° - i.
\end{aligned}
\tag{A.2}
$$

Using the cosine law for spherical triangles (see e.g. Smart (1977)), the angle B_0 can thus be computed from the rotation elements:

$$\sin B_0 = sin(\eta - \Omega) \sin i \tag{A.3}$$

Now consider the angle made by the projection of the rotation axis CP onto the plane of the disk, and the pole of the ecliptic CK. Let us denote this angle[3] by y (see figure A.2). The axes CE, CT, and CK define a rectangular coordinate system, and the coordinates of P are given by $(\sin KP \cos EF, \sin KP \sin EF, \cos KP)$. Hence the projection of P onto the CT-CK plane has coordinates $(\sin KP \sin EF, \cos KP)$, and the angle y is given by $\tan y = \tan KP \sin EF$. The angle KP is the inclination i, and EF can be expressed in terms of Ω such that

$$\tan y = -\cos(\eta - \Omega) \tan i \tag{A.4}$$

Equations A.3 and A.4 thus define the coordinate system on the disk as seen from Earth.

A.2 SOHO Orbit and Alignment

The SOHO spacecraft orbits the Sun in a halo orbit about the Earth-Sun Lagrange point L_1. The spacecraft attitude is maintained (via star trackers) so that the MDI camera is aligned always with the Carrington rotation elements. More precisely, if the Sun's rotation axis is accurately described by the elements (i_c, Ω_c) of equation A.1, then SOHO is aligned such that the angle y described by equation A.4 will always be zero.

On the other hand, what if the Sun rotates about an axis described by coordinates (i, Ω) which are slightly different from the Carrington elements? Clearly this will mean that the position angle y and the heliographic latitude of disk center B_0 will be somewhat different from their expected values. To quantify these effects, suppose that the actual rotation elements of the Sun differ from the Carrington elements according to

[3]Note that y is *not* the position angle P of the rotation axis as it is usually defined.

$$\begin{aligned} i &= i_c + \Delta i, \\ \Omega &= \Omega_c + \Delta\Omega. \end{aligned} \tag{A.5}$$

Define the angle errors

$$\begin{aligned} E_P &\equiv y - y_c, \\ E_B &\equiv B_0 - B_{0c}. \end{aligned} \tag{A.6}$$

Here y_c is given by equation A.4, with i replaced by i_c and Ω replaced by Ω_c. The latitude B_{0c} is defined in the same way by equation A.3.

Using Taylor series expansions for the trigonometric functions, the equations A.3 and A.4 can be used to express y and B_0 in terms of the known values y_c and B_{0c} and the errors Δi and $\Delta\Omega$. The definitions A.6 can then be used to write

$$E_P \simeq \frac{-(\Delta\Omega \tan i_c \sin(\eta - \Omega_c) + \Delta i \sec^2 i_c \cos(\eta - \Omega_c))}{1 + \tan^2 i_c \cos^2(\eta - \Omega_c)} \tag{A.7}$$

$$E_B \simeq \frac{\Delta i \cos i_c \sin(\eta - \Omega_c) - \Delta\Omega \sin i_c \cos(\eta - \Omega_c)}{[1 - \sin^2 i_c \sin^2(\eta - \Omega_c)]^{1/2}} \tag{A.8}$$

Here all terms which are second-order or higher in Δi, $\Delta\Omega$, E_P, and E_B have been neglected, since all of these quantities can be assumed to be quite small. Furthermore, the quantity i_c is small enough that terms which are second-order in i_c can also be ignored; in this case equations A.7 and A.8 simplify to

$$E_P \simeq -(\Delta\Omega \tan i_c \sin(\eta - \Omega_c) + \Delta i \cos(\eta - \Omega_c)) \tag{A.9}$$

$$E_B \simeq \Delta i \cos i_c \sin(\eta - \Omega_c) - \Delta\Omega \sin i_c \cos(\eta - \Omega_c) \tag{A.10}$$

Hence it can be seen that the angle errors E_B and E_P will vary with a one-year period as SOHO orbits around the Sun. This fact provides the basis for the measurement of Δi and $\Delta\Omega$ outlined in the following section. It is worth noting that some other sources of these angle errors — for example, a fixed error in the alignment of MDI relative to the SOHO axis — do *not* show a similar dependence on orbital position.

A.3 Solar Velocities and Angle Errors

An error in the position angle or in the heliographic latitude of disk center will result in errors in the analysis of solar velocities. For example, if the position angle has a small error E_P, then the "meridional" velocity determined in the analysis will contain a component of the zonal velocity or rotation which leaks in:

$$v_{\theta,m}(\theta) = v_\theta(\theta) + v_\phi(\theta) \sin E_P \tag{A.11}$$

Here the subscript m denotes a measured velocity, whereas values without such notation are the true velocities in the θ and ϕ directions. For the rotation, the principal source of error will be a misidentification of the latitude of each position on the disk:

$$v_{\phi,m}(\theta) = v_\phi(\theta) - v'_\phi(\theta) E_B \tag{A.12}$$

where v'_ϕ is the derivative of the zonal velocity with respect to colatitude θ. The minus sign in equation A.12 arises because the error E_B is defined as a latitude error, while the derivative is made with respect to the colatitude.

Since the errors E_B and E_P which arise from an error in the Carrington elements vary during the orbit of SOHO, it should be possible to extract them from the measured velocities. For this purpose, a time series of velocities was constructed, with two average profiles $v_\theta(\theta)$ and $v_\phi(\theta)$ for each Carrington rotation. The total length of the time series was somewhat more than two years. For the first iteration of the procedure, the true rotation profile $v_\phi(\theta)$ was taken to be the mean of the measured profiles. A function of the form

$$v(\eta - \Omega_c) = a_0 + a_1 \sin(\eta - \Omega_c) + a_2 \cos(\eta - \Omega_c) \tag{A.13}$$

was then fit to each of $v_{\phi,m}$ and $v_{\theta,m}$ at each colatitude by a linear least-squares method. Combining equations A.11 and A.9, it was possible to determine

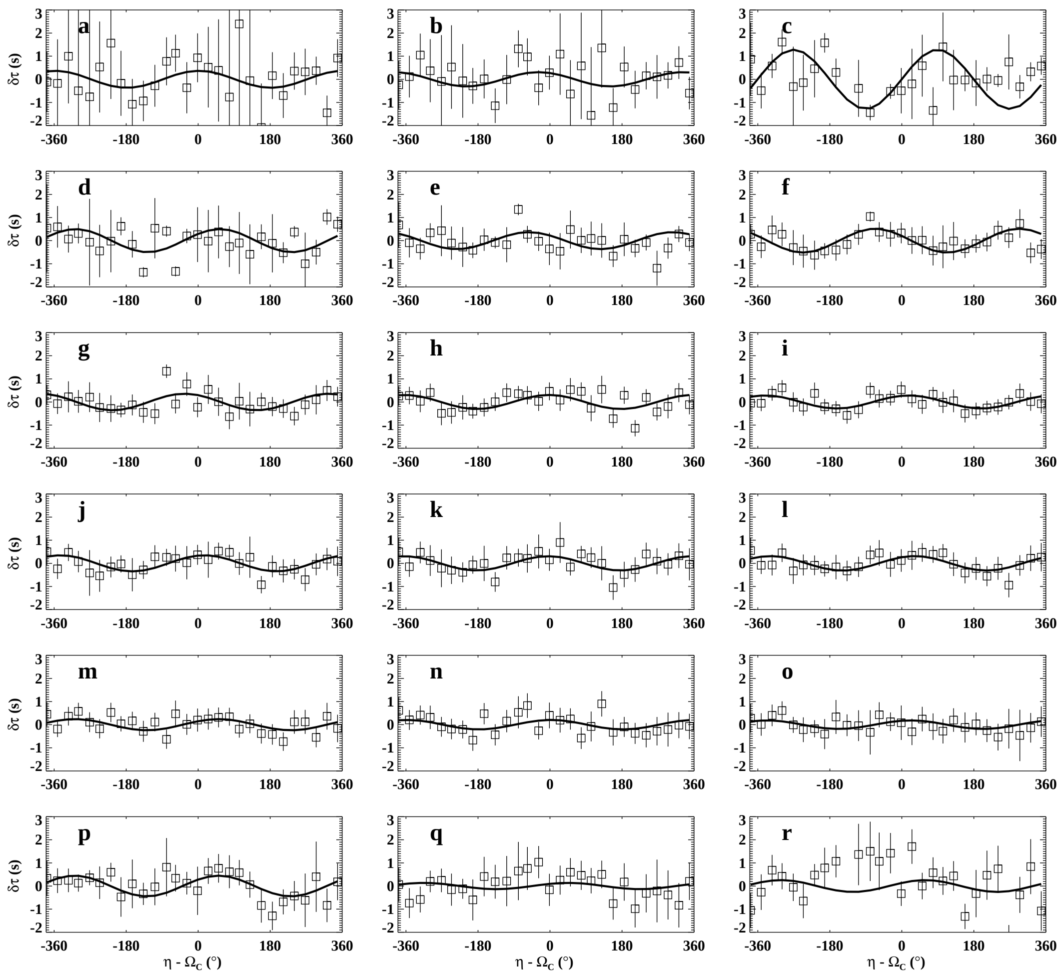

Figure A.3: The time variation of the meridional velocity is plotted for eighteen different latitudes. The horizontal axis denotes the coordinate $\eta - \Omega_c$, where η is the SOHO-centric longitude of the Sun, and Ω_c is defined in equation A.1. The vertical axis shows the difference $\delta\tau$ between the southward and northward travel times for travel distances of 3° to 10°. In each plot, the mean value of the velocity has been removed in order to emphasize the time variation. A positive time difference represents a meridional flow more northward than the mean. The squares represent the measured data points, where there is one point for each Carrington rotation. The solid curve is a function of the form given in equation A.13. The latitudes and fit parameters are summarized in table A.1.

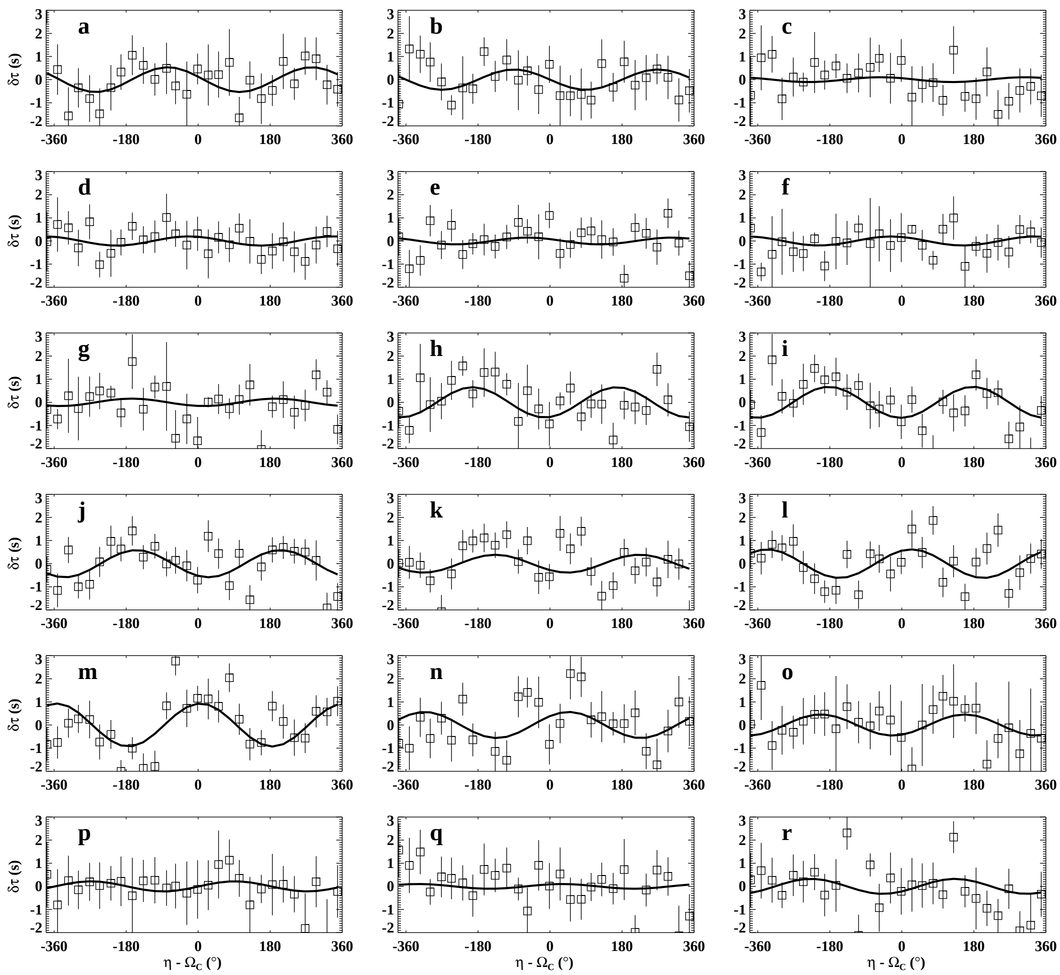

Figure A.4: The time variation of the rotation is plotted for eighteen different latitudes. The horizontal axis denotes the coordinate $\eta - \Omega_c$, where η is the SOHO-centric longitude of the Sun, and Ω_c is defined in equation A.1. The vertical axis shows the difference $\delta\tau$ between the eastward and westward travel times for travel distances of $3°$ to $10°$. In each plot, the mean value of the velocity has been removed in order to emphasize the time variation. A positive time difference represents a rotation velocity which is faster than the mean. The squares represent the measured data points, where there is one point for each Carrington rotation. The solid curve is a function of the form given in equation A.13. The latitudes and fit parameters are summarized in table A.2.

$$
\begin{aligned}
\langle v_\theta \rangle &= a_0, \\
\Delta\Omega &= -\frac{a_1}{v_\phi \tan i_c}, \quad \text{and} \\
\Delta i &= -\frac{a_2}{v_\phi}
\end{aligned}
\tag{A.14}
$$

from $v_{\theta,m}$ at each colatitude. Similarly, estimates for Δi and $\Delta\Omega$ can be made from the measurements of the zonal velocities:

$$
\begin{aligned}
\langle v_\phi \rangle &= a_0, \\
\Delta i &= -\frac{a_1}{v'_\phi \cos i_c}, \quad \text{and} \\
\Delta\Omega &= \frac{a_2}{v'_\phi \sin i_c}
\end{aligned}
\tag{A.15}
$$

At every latitude, a time series of time differences was constructed with one point for each of 28 Carrington rotations. A function of the form of equation A.13 was fit to the time series using a weighted least squares technique. Figures A.3 and A.4 show the time series and fits. The measurement errors used in the fitting were calculated as described in section 4.5. The values of Δi and $\Delta\Omega$ were derived from the parameters of the least-squares fit, along with uncertainties; these values are given in tables A.1 and A.2.

From the measurements of the meridional flow, the mean values of these quantities were $\Delta i = -(0.091 \pm 0.012)^\circ$, and $\Delta\Omega = -(0.18 \pm 0.10)^\circ$. Slightly different values were obtained from the rotation meaurements: $\Delta i = -(0.105 \pm 0.033)^\circ$ and $\Delta\Omega = (0.16 \pm 0.27)^\circ$. Thus the two measurements agree with one another within their uncertainties; however, it there are clearly some systematic errors in the measurements derived from the zonal velocity. Table A.2 shows that the values for both Δi and $\Delta\Omega$ show a sytematic dependence on latitude, being especially large in magnitude near the equator. The plots in figure A.5 show that while the measurements made using meridional flows are normally distributed about their mean values, the measurements made from zonal flows are widely (and not randomly) scattered. The most extreme

Fig.	λ (°)	χ^2	Δi(°)	$\Delta\Omega$(°)
a	-42.5	0.5	-0.190±0.157	-0.052±1.831
b	-37.4	0.5	-0.127±0.107	0.545±1.132
c	-32.6	6.2	-0.005±0.061	-4.385±0.617
d	-27.4	3.4	-0.119±0.049	-1.282±0.498
e	-22.5	1.3	-0.085±0.047	0.885±0.410
f	-17.7	0.8	-0.075±0.044	1.377±0.394
g	-12.7	1.0	-0.107±0.042	0.571±0.386
h	-7.5	0.9	-0.108±0.037	0.038±0.325
i	-2.4	0.5	-0.094±0.033	-0.238±0.279
j	2.4	0.5	-0.118±0.044	-0.257±0.354
k	7.5	0.5	-0.109±0.049	0.065±0.374
l	12.7	0.4	-0.096±0.044	-0.471±0.349
m	17.7	0.6	-0.055±0.042	-0.549±0.342
n	22.5	0.6	-0.078±0.048	-0.024±0.420
o	27.4	0.2	-0.069±0.058	-0.223±0.478
p	32.6	0.5	-0.121±0.070	-1.194±0.564
q	37.4	0.5	-0.045±0.086	-0.357±0.758
r	42.5	1.8	-0.070±0.099	-0.889±0.923
Means			-0.091±0.012	-0.182±0.101

Table A.1: Determination of elements i and Ω from meridional velocity. Each row in the table corresponds to a plot in figure A.3. The quantities Δi and $\Delta\Omega$ were estimated from each plot independently as described in the text. The last row gives the mean values for Δi and $\Delta\Omega$, where each measurement has been appropriately weighted according to its uncertainty.

deviations from the mean values are for latitudes near the equator (plots h, i, j, k, l, and m of figure A.4 and table A.2. When these measurements are excluded from the mean, the values for Δi and $\Delta\Omega$ become (-0.112 ± 0.034) and (-0.28 ± 0.28), respectively. However, it is at least slightly dubious to suggest that there exists a systematic error which causes only these particular measurements to be incorrect. Until the source of this one-year oscillation in the zonal velocity is explained, it is probably safest to disregard the measurements from zonal velocities altogether.

Fig.	λ (°)	χ^2	Δi(°)	$\Delta\Omega$(°)
a	-42.5	0.9	-0.208±0.099	-0.404±0.732
b	-37.4	0.7	-0.208±0.102	0.002±0.846
c	-32.6	0.7	-0.043±0.108	-0.253±0.895
d	-27.4	0.5	-0.045±0.113	-0.816±0.885
e	-22.5	1.3	-0.088±0.125	-0.472±0.937
f	-17.7	1.3	-0.093±0.188	-1.454±1.104
g	-12.7	1.1	-0.060±0.279	1.918±1.763
h	-7.5	2.0	0.365±0.473	12.565±3.365
i	-2.4	1.5	0.145±1.036	29.495±7.802
j	2.4	1.6	1.612±1.010	-26.241±7.708
k	7.5	2.3	0.546±0.342	-4.524±2.564
l	12.7	1.6	-0.399±0.280	7.207±2.069
m	17.7	2.4	-0.101±0.206	8.330±1.477
n	22.5	1.6	-0.288±0.163	2.158±1.240
o	27.4	0.6	-0.101±0.159	-1.897±1.309
p	32.6	0.2	-0.112±0.132	-0.035±1.138
q	37.4	0.9	-0.024±0.096	0.328±0.893
r	42.5	1.7	-0.099±0.086	-0.724±0.804
Means			-0.105±0.033	0.166±0.269

Table A.2: Determination of elements i and Ω from zonal velocity. Each row in the table corresponds to a plot in figure A.4. The last row gives the mean values for Δi and $\Delta\Omega$, where each measurement has been appropriately weighted according to its uncertainty.

A.4 Previous Results and Discussion

Prior to 1975, every determination of the rotation elements i and Ω relied on essentially the same method used by Carrington. The approach used is to observe the motions of a large number of sunspots (over a long time period), and to use those motions to infer the direction of the axis of rotation. The approach relies on the assumption that, averaged over these long time periods (typically several years), sunspots do not exhibit significant asymmetric meridional motions. In the early part of this century, attempts to measure the rotation elements were made by Dyson &

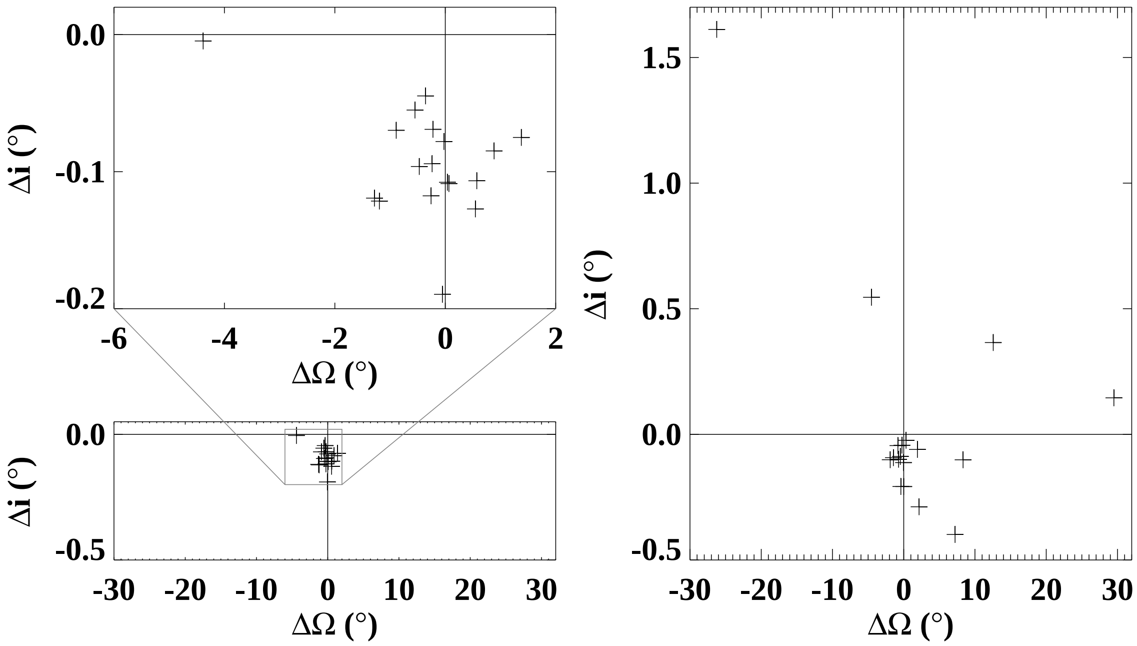

Figure A.5: The measurements from tables A.1 and A.2 have been plotted in the (i, Ω) phase space. The left-hand pair of figures is for the measurements made using the meridional flows; the right-hand figure is for the measurements of zonal flows. The lower plot on the left is on the same scale as the right-hand plot, to demonstrate the relative scatter of the two sets of measurements. The upper plot on the left shows a close-up of the meridional measurements.

Maunder (1912; 1913) and by Epstein (1916; 1917). None of these works (or Carrington's) offered any estimate of the uncertainty in their calculated values.

More recent efforts using sunspots have been made by Balthasar *et al.* (1986; 1987), by Stark & Wöhl (1981), and by Clark (1979). These four results agree with each other reasonably well (see figure A.6) and show that the inclination i is somewhat less than i_c, whereas the longitude defined by Ω is somewhat larger than Ω_c. As an interesting sidenote, the paper by Stark and Wöhl includes a recalculation of i_c and Ω_c from Carrington's original data, and estimates their uncertainties to be at least $\pm 0.11°$ and $\pm 0.52°$ respectively.

In the last few decades, some attempts have been made to determine the rotation

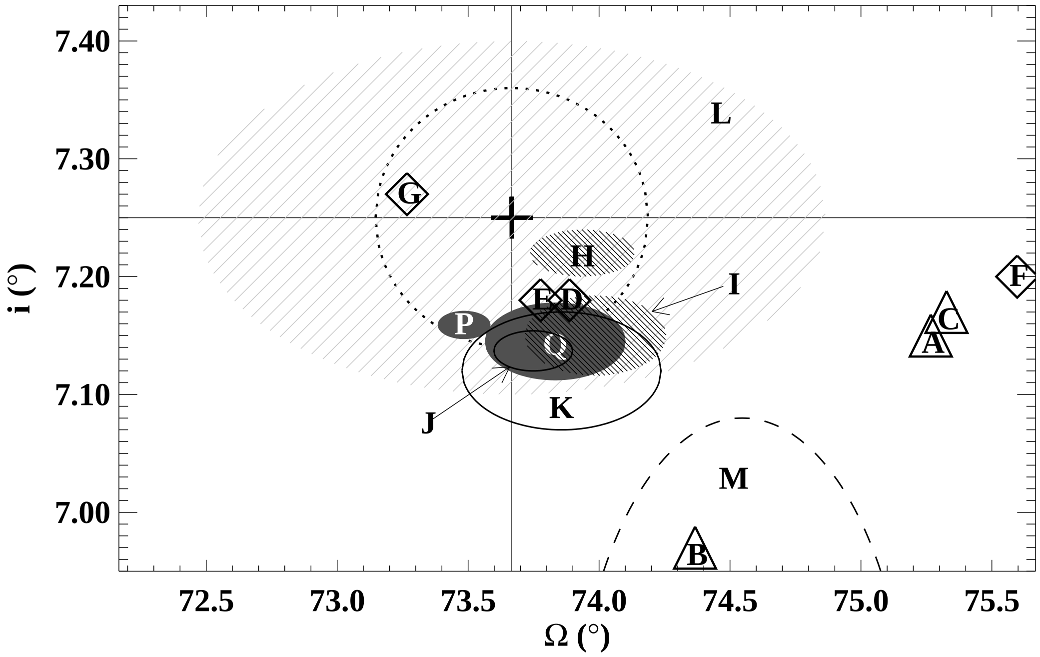

Figure A.6: A collection of past measurements of i and Ω. Note that Ω shown here is the value for year 1850.0. The "standard" values used (marked by the cross) are those given by Carrington (1863); the region marked by the dotted line represents an estimate of the uncertainty in Carrington's measurement, made by Stark and Wöhl (1981) using Carrington's original data. The triangles represent other measurements made during the nineteenth century, all from measurements of sunspots: (A) Laugier (1840); (B) Spoerer (1866); (C) Wilsing (1882). These three measurements are taken as cited by Wöhl (1978), who also includes a more complete selection of early measurements (these do not appear within the range of this plot). The four diamonds represent slightly more modern measurements, also from sunspots: (D) Dyson and Maunder (1912); (E) Dyson and Maunder (1913); (F) Epstein (1916); (G) Epstein (1917). The rest of the measurements, which are even more recent, include estimates of the uncertainty and are therfore depicted as ellipses of the appropriate size. Four of these are also from sunspot measurements: (H) Clark *et al.* (1979); (I) Stark and Wöhl (1981); (J) Balthasar *et al.* (1986); (K) Balthasar *et al.* (1987). The two largest ellipses are for measurements using direct Doppler velocities: (L) Labonte (1981) and (M) Wöhl (1978). The results from this work are the filled ellipses denoted by P (from the meridional circulation) and Q (from the rotation).

elements from direct Doppler measurements (Wöhl, 1978; LaBonte, 1981). Since it has long been observed that sunspots rotate at a slightly different *rate* than the bulk plasma (see the excellent review by Beck (2000) for examples), the question has been raised whether the rotation *axis* of the sunspots might also be different from that of the plasma. The result of Wöhl (1978) suggests that the rotation elements measured from Doppler velocites are significantly different from the magnetic measurements, although he attributes this to a probable error in the Carrington elements rather than the existence of two different axes of rotation. LaBonte (1981) found that the elements measured from Mt. Wilson data did not differ from the Carrington elements to within the uncertainty of his observations. It is worth noting that of all of the modern measurements shown in figure A.6 the two determinations from Doppler observations show the largest uncertainties. It is probably only possible to say that the "two-axis" question remains unanswered, although any difference between the hypothetical axes is certainly quite small.

The measurements presented in this work are not subject to many of the same systematic effects of earlier work. In particular, no assumptions are made about the north-south symmetry of either the rotation or the meridional flow. In fact, after removing the time-varying signals E_P and E_B the meridional flow still shows a significant southward bias over the duration of the observations. On the other hand, any *real* time-variation in the flow could be confused with the error signal. Since the observing period is only twice the period of the expected error signal, it is possible that the real time variation is not being separated very well from the spurious one. Also, there are probably some small systematic errors which arise from the time-distance treatment of the measurements. However, it should be noted that at only one point is a velocity converted to a travel-time difference or vice versa, and that is in the computation of v_ϕ to use in equations A.11 and A.12. As a final note, the measurements presented in this work depend on the assumption that the SOHO spacecraft pointing was constant during the entire observing run. Although this may not be strictly true, it is unfortunately the best information currently available. In the future, more accurate orientation information may be available from the spacecraft log files, at which time the estimates here might be revised.

Figure A.6 shows clearly that the set of modern measurements supports a value of i which is significantly less than i_c; a consensus seems to indicate a value of $i = 7.15°$. The measurements of Ω are of course subject to much greater uncertainty than the measurements of i, owing to the small value of the latter coordinate. The collection of modern measurements is consistent with the conclusion that $\Omega = \Omega_c$, at least to within twice the measurement uncertainty.

A.5 Conclusions

I have presented time-distance measurements of the meridional and zonal flows on the Sun which show time variations with periods which match the orbital period of the SOHO spacecraft. The time variation in the meridional velocity is consistent with an error in the Carrington elements of $\Delta i = -(0.091 \pm 0.012)°$, and $\Delta\Omega = -(0.18 \pm 0.10)°$. The time variation in the zonal velocity is more problematic, since it contains some spurious time variation which cannot be explained by this effect. However, a selected subset of measurements appear to also be consistent with the above error in the Carrington elements. The corrected values of the Carrington elements are in good general agreement with modern measurements, and indeed are within the (unstated) uncertainties in Carrington's original measurements (Stark and Wöhl, 1981).

These measurements using MDI data give an uncertainty in the Carrington elements which is smaller than any previous result. The evidence is very strong that the rotation axis of the Sun is inclined to the plane of the ecliptic by less than $i_c = 7.25°$; I suggest that a new value of $i = 7.15°$ be adopted, based on the collection of all the measurements which have been made to date.

In terms of the other results presented in this thesis, this conclusion obviously must be taken into consideration when examining time variation of solar flows. For the measurements presented in section 6.2.4, most of the apparent time variation in the equator-crossing flow can be accounted for by the error in the solar inclination.